Article

Binding Study of Antibacterial Drug Ciprofloxacin with Imidazolium-Based Ionic Liquids Having Different Halide Anions: A Spectroscopic and Density Functional Theory Analysis

Abrar Siddiquee, Zahoor Parray, Aashima Anand, Shadma Tasneem, Nazim Hasan, Waleed M. Alamier, Abeer A. Ageeli,* Farooq Ahmad Wani, Prashant Singh, and Rajan Patel*

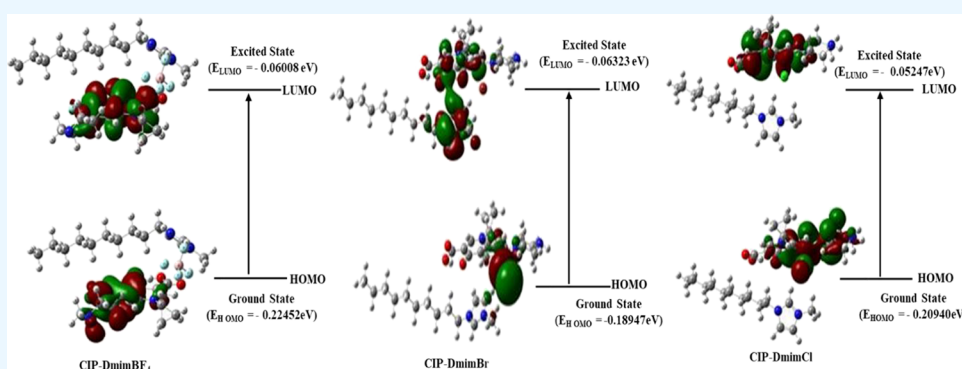Cite This: *ACS Omega* 2023, 8, 42699−42710

Read Online

ACCESS | ▮▮▮ Metrics & More | ▤ Article Recommendations | ⓢ Supporting Information

ABSTRACT: Herein, we have shown the interaction of an antibiotic drug ciprofloxacin (CIP) with three surface-active ionic liquids (ILs), having the same cation and different anions, namely, 1-decyl-3-methylimidazoliumtetrafluoroborate $[C_{10}mim][BF_4]$, 1-decyl-3-methylimidazolium bromide $[C_{10}mim][Br]$, and 1-decyl-3-methylimidazolium chloride $[C_{10}mim][Cl]$. This study has been performed by exploiting various spectroscopic techniques such as steady-state fluorescence, time-resolved fluorescence, and UV−visible spectroscopy. The fluorescence emission study of CIP with ILs was performed at various concentrations of all the three ILs. The emission spectra of CIP decreased in the presence of ILs, suggesting complex formation between CIP−IL. The effect of different concentrations of ILs on the emission spectra of CIP was exploited in terms of quenching and binding parameters. Further, fluorescence emission study was validated by the time-resolved fluorescence technique by measuring the average lifetime (τ_{avg}) of CIP in the presence of all the three ILs. The τ_{avg} value of the drug changed with the addition of ILs, which suggests complex formation between the drug and ILs. This complex formation was also confirmed by UV−visible spectroscopy results of CIP with all the three ILs. Further, for evaluating the thermodynamic parameters of the CIP−IL interactions, isothermal titration calorimetry (ITC) was performed. The ITC experiment yielded the thermodynamic parameters, ΔH (change in the enthalpy of association), ΔG (Gibbs free energy change), ΔS (entropy change), and binding constant (K_a). The binding parameters driven by ITC revealed that CIP−IL interactions are spontaneous in nature and enthalpy-driven, involving hydrophobic forces. Further, the classical density functional theory (DFT) calculations were performed, which provided deep insight for CIP−IL complex formation.

1. INTRODUCTION

The solubility of drugs is a major concern for the pharmaceutical industry and chemical scientists in the past several years. Adequate solubilization of the drug is the most challenging aspect for drug delivery.[1,2] This difficulty has driven pharmaceutical researchers to develop new methods or approaches to formulating drugs.[3,4] Various attempts have been made to enhance drug solubility at the time of drug formulation, some of which include salt formation, tailoring of active pharmaceutical ingredients (APIs), and complex formation with surface active molecules.[5−7] In many cases, even these approaches cannot completely overcome the solubility-related troubles.[3,8] Therefore, it becomes necessary

to modify the traditional techniques for an effective drug formulation and its site-specific delivery.[3,9−11] Surface active ionic liquids (ILs) show the most fascinating properties to address these issues.[12−15] Therefore, ILs are being probed as alternative materials and solvents in various ranges of applications including biotechnology, pharmaceutics, and
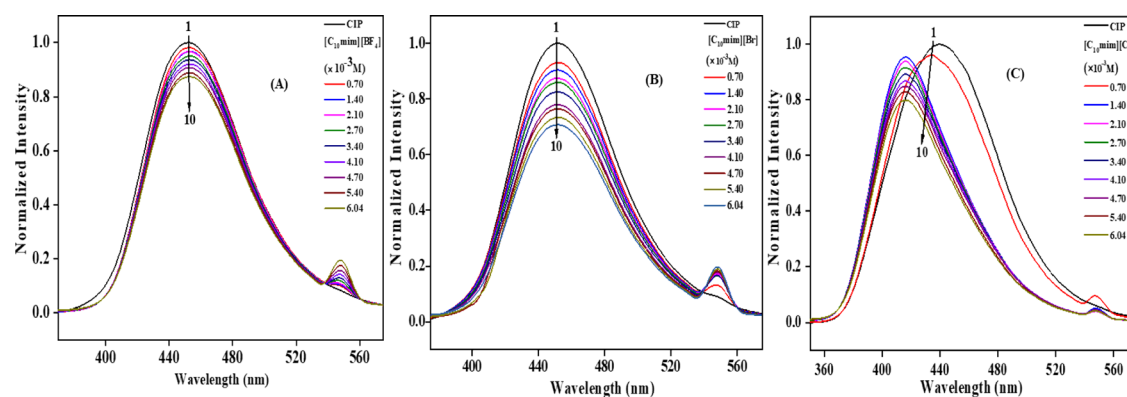
Figure 1. Fluorescence emission spectra of CIP (20 μM, λ_{max} = 274 nm) in the presence of $[C_{10}mim][BF_4]$ (A), $[C_{10}mim][Br]$ (B), and $[C_{10}mim][Cl]$ (C).

antimicrobial agents.[16−18] ILs enhance the transportation of drugs to the site of action, and hence, they emerged as novel drug delivery agents.[19] Recently, ILs have been actively utilized in modifying drugs' physicochemical properties such as suspension rate, permeability, and bioavailability.[20,21]

ILs are organic salts having outstanding physical properties, which make these ideal competitors in several fields including biological and pharmaceutical sciences.[7,17,22] ILs have insignificant vapor pressure, high conductivity, and thermal stability and are miscible with a wide range of solvents, including water.[23−27] By tuning their cations or anions, ILs can be effortlessly designed as task-specific ILs and hence can be considered as "designer solvents".[27−29] Modulating the structure of ILs' cation or the counterion, ILs have displayed higher physiochemical and biological properties and the complexation of ILs with API can improve the solubility, bioavailability, and activity of the drug.[30] These exceptional properties of ILs open wide choices for their applications in the pharmaceutical industry. Several drug-based IL conjugates and their synergistic interactions have been reported in the literature.[16,17,31−33] The outcomes have suggested that IL−drug complexation enhanced the solubility and bioavailability of poorly soluble drugs.[20,31,34−36] Sintra et al. have reported the solubility of the drug ibuprofen in the presence of ILs. The results revealed that the complexation of ibuprofen−IL enhanced the solubility of the pure drug in aqueous medium.[34] In another report, Huang et al. studied the interaction of a poorly soluble drug with sodium dodecyl sulfate (SDS). They demonstrated that the solubility of the drug elevated in SDS solution through the formation of ion pairs between the drug and the aqueous solution of SDS.[37] Reid et al. demonstrated the antimicrobial activity of a series of ILs in terms of minimum inhibitory concentration (MIC). They correlated the counterion structure and hydrophobicity with the MIC value of the tested ILs. Results revealed that higher hydrophobic IL displayed a lower MIC value against clinically accepted microorganisms.[38]

Recently, Ghosh et al. explored the adsorption and separation of a fluoroquinolone drug at the air−water interface by using ionic surfactants (CTAB/SDS). They found that poorly water-soluble drugs have higher removal efficiency with SDS than with CTAB. The adsorption of poorly soluble drugs was due to complexation between the drug and the surfactant through ion-pair formation.[39] Kurnik et al. developed cholinium-IL-based amphiphilic polymeric micelles by utilizing Pluronic and various ILs in biphase micellar systems for

hydrophobic drug delivery. Their investigation suggested that surface-active molecules have a strong affinity to solubilize sparingly soluble drugs.[40] Therefore, a deeper investigation of IL and drug interaction is necessary to understand their physiochemical behavior. In this regard, we have tried to explore the interaction of the antibacterial drug ciprofloxacin and surface-active ILs 1-decyl-3-methylimidazolium tetrafluoroborate $[C_{10}mim][BF_4]$, 1-decyl-3-methylimidazolium bromide $[C_{10}mim][Br]$, and 1-decyl-3-methylimidazolium chloride $[C_{10}mim][Cl]$ in aqueous medium.

Ciprofloxacin (CIP) is an antibacterial drug of second generation, which displays exceptional pharmacokinetic and antimicrobial properties. It is an extensively prescribed fluoroquinolone antibiotic and is widely utilized for the treatment of urinary, skin, and other bacterial diseases.[41,42] Due to its widespread use, the proportion of its resistance (drug resistance) is exponentially increasing and, thus, the development of a new or improved therapeutic regimen that works against its resistance is necessary.[43,44] The present research work is explored using various spectroscopic techniques such as steady-state fluorescence, time-resolved fluorescence, UV−visible spectroscopy, and calorimeter techniques like isothermal titration calorimetry (ITC) techniques. The results have been investigated to gain insight into the nature of the anions of imidazolium-based ILs and their binding with the drug. The spectroscopy results are supplemented by classical density functional theory (DFT) calculations. This study may be helpful in the formulation of API-IL-based antibacterial drugs.

2. RESULTS AND DISCUSSION

2.1. Steady-State Fluorescence Spectroscopy. The quantitative interactions of CIP with ILs have been explored by a fluorescence emission spectroscopy technique. The emission spectra of CIP in the absence and presence of all the three ILs were recorded at 274 nm.[45,50] Figure 1A−C shows the emission spectra of CIP (20 μM) in the absence and presence of $[C_{10}mim][BF_4]$, $[C_{10}mim][Br]$, and $[C_{10}mim][Cl]$, respectively. The spectra given in Figure 1 revealed that the emission spectrum of CIP gets quenched progressively upon the successive addition of each IL in increasing concentrations. The quenching in the emission spectra of CIP in the presence of ILs suggests the complex formation between CIP−IL through attractive forces due to ion pairs.[51] The complexation of drug with IL molecules involved cation−π interaction between the imidazolium cation and CIP. The emission
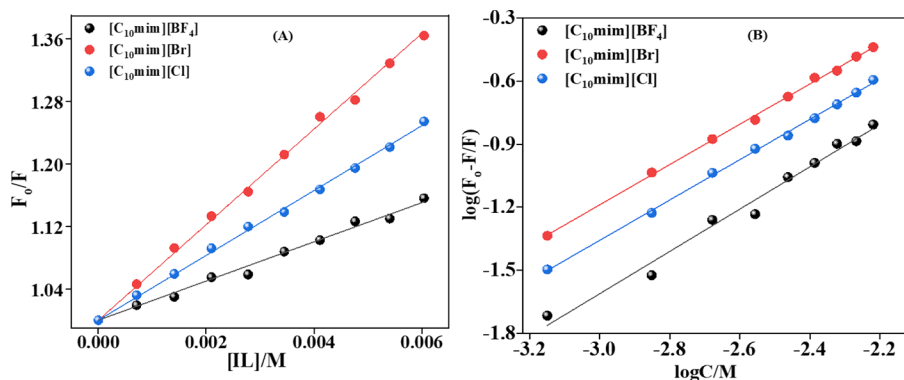
Figure 2. Stern−Volmer plots (A) and plots of $\log(F_0 - F/F)$ vs $\log C$ (B) of CIP in the presence of $[C_{10}mim][BF_4]$, $[C_{10}mim][Br]$, and $[C_{10}mim][Cl]$.

Table 1. Stern−Volmer Quenching Constants (K_{sv}), Binding Constant (K_b), Number of Binding Sites (n), and Corresponding Gibbs Free Energy (ΔG) for CIP−IL Complexes

system	K_{sv} (L mol^{-1})	K_q (L mol^{-1} S^{-1}) ($\times 10^{10}$)	K_b (L mol^{-1})	ΔG (kJ/mol)	n
CIP-$[C_{10}mim][BF_4]$	61.20	5.36	48.62	−9.62	1.00
CIP-$[C10mim][Br]$	41.50	3.64	33.11	−8.67	0.95
CIP-$[C10mim][Cl]$	25.09	2.20	25.56	−8.03	0.95

spectra of CIP in the presence of $[C_{10}mim][Cl]$ showed a blue shift, which could be attributed to the complex formation between CIP and $[C_{10}mim][Cl]$, predominantly by hydrophobic forces. The occurrence of a blue shift indicates that the polarity around the drug molecule continuously changed and the drug experienced a more hydrophobic environment.

The emission study of CIP at various concentrations of $[C_{10}mim][BF_4]$, $[C_{10}mim][Br]$, and $[C_{10}mim][Cl]$ and the corresponding changes in the emission spectra were analyzed according to the Stern−Volmer equation, given by eq 1.

$$\frac{F_0}{F} = 1 + K_{sv}[Q] = 1 + k_q \tau_0[Q] \tag{1}$$

where F_0 and F are the fluorescence intensities of CIP in the absence and presence of the quencher, respectively, K_{sv} is the Stern−Volmer quenching constant, and $[Q]$ is the quencher (ILs) concentration. The linear fitting of the plot of F_0/F vs IL concentration is given in Figure 2A, and according to eq 1, utilizing the value of slope yielded K_{sv}, the values of which are given in Table 1 for all the three ILs. From Table 1, it is revealed that the K_{sv} value increases in the order $[C_{10}mim][BF_4] > [C_{10}mim][Br] > [C_{10}mim][Cl]$.

Further, to find the type of quenching mechanism involved in the study, we calculated the quenching rate constant (k_q) for the CIP−IL binding systems by using K_{sv} and the average fluorescence lifetime (τ_o) value by using the relation $k_q = \frac{K_{sv}}{\tau_o}$. The τ_o value of pure CIP was found to be 1.14 ns as given in Table S1. The values of k_q for the binding between CIP and $[C_{10}mim][BF_4]$, $[C_{10}mim][Br]$, and $[C_{10}mim][Cl]$ are given in Table 1. The values mentioned in Table 1 were found to be higher than the value of the maximum diffusion collision quenching rate constant (2×10^{10} L mol^{-1} s^{-1}), which signifies that the quenching was mainly being governed by a static mechanism. This quenching mechanism was further confirmed by time-resolved fluorescence measurements (Section 2.2). Fluorescence binding study of CIP with different ILs revealed that the structural change in the counterion in the IL plays a vital role in the binding and that the BF$_4^-$ anion has more

quenching ability than Br$^-$ and Cl$^-$ ions. There is a subtle interplay of the hydrophobic and electrostatic interactions as well as hydrogen bonding, which decides the complexation of drug with ILs.[52,53] To check the binding affinity of CIP with all three ILs, the binding constant (K_b) and the number of binding sites (n) were calculated by utilization of the fluorescence emission spectroscopic study. K_b and n were obtained from the linear fitting of the plot of $\log(F_0 - F/F)$ vs $\log[IL]$ (Figure 2B) according to eq 2.

$$\log\frac{(F_0 - F)}{F} = \log K_b + n\log[Q] \tag{2}$$

where n is the number of binding sites, and K_b is the binding constant. The symbols F_0 and F have the same meanings as those in eq 1.

The value of K_b was obtained by utilizing the intercept, while the slope gave n from the linear fitting of $\log(F_0 - F)/F$ vs $\log[IL]$ plots. All of the calculated values of K_b and n for CIP and IL interactions are summarized in Table 1. From Table 1, it can be seen that CIP binds strongly with all three ILs. However, IL having a BF$_4^-$ ion binds strongly with CIP than ILs having Br$^-$ and Cl$^-$ ions.[54] It may be due to the greater degree of hydrogen bonding between CIP and the BF$_4^-$ ion of the IL. Further, the average value of n per molecule is close to 1 for all three ILs, which suggests that interaction of CIP with IL might involve 1:1 binding. Moreover, Gibbs free energy change (ΔG) for CIP and IL interactions was calculated by using the following relation 3.

$$\Delta G = -RT\ln K_b \tag{3}$$

ΔG values for all the systems are given in Table 1, and they suggested that the complexation of CIP with $[C_{10}mim][BF_4]$, $[C_{10}mim][Br]$, and $[C_{10}mim][Cl]$ is spontaneous. The ΔG value is higher for CIP-$[C_{10}mim][BF_4]$ than for CIP-$[C_{10}mim][Br]$ and $[C_{10}mim][Cl]$. The unusual behavior of $[C_{10}mim][BF_4]$ with drug binding suggests that the drug has more binding affinity with tetrafluoroborate counterions than with bromide- or chloride-containing imidazolium cations.
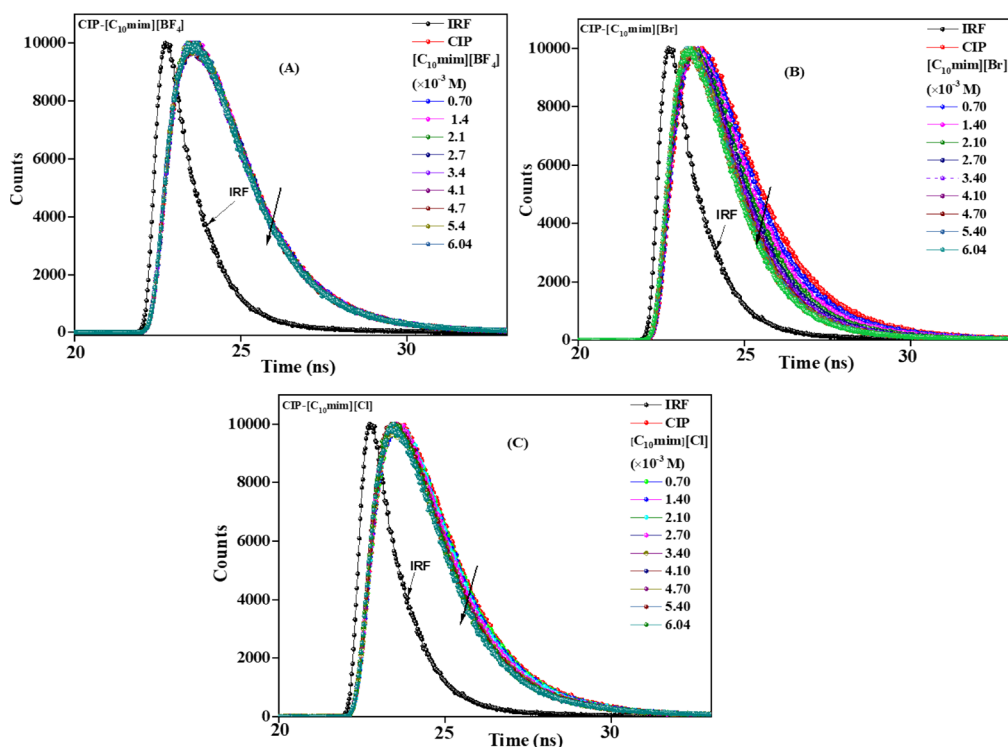
Figure 3. Time-resolved fluorescence spectra of CIP (20 μM) in the presence of $[C_{10}mim][BF_4]$ (A), $[C_{10}mim][Br]$ (B), and $[C_{10}mim][Cl]$ (C).
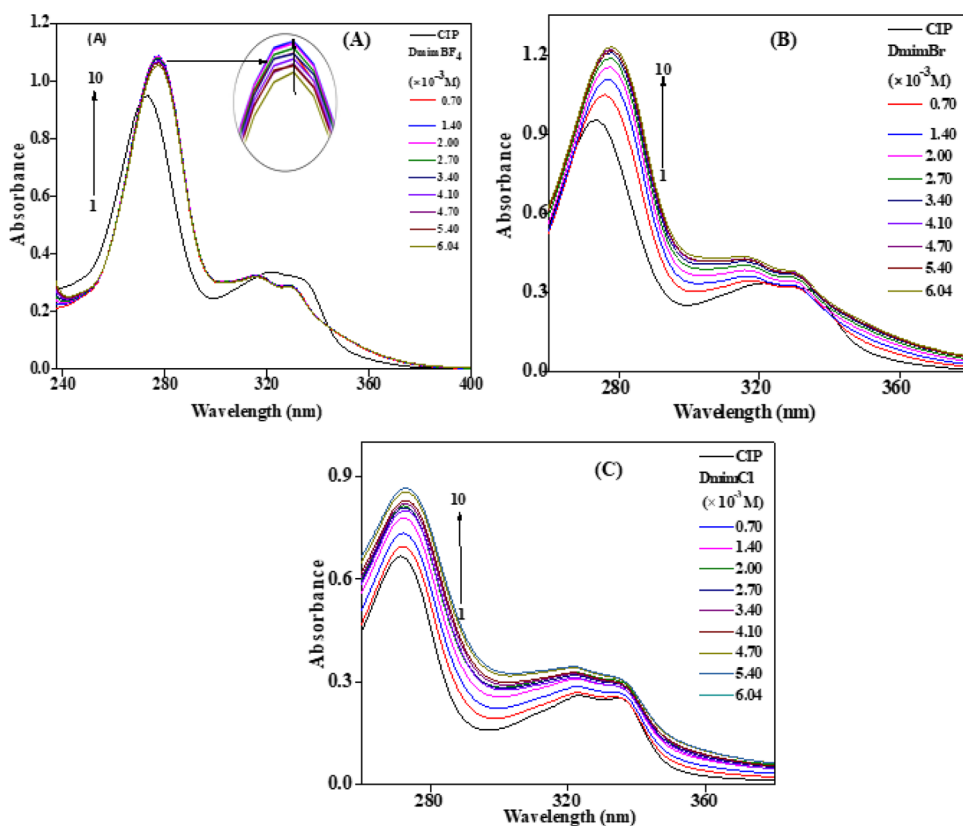
Figure 4. Absorption spectra of CIP (20 μM) as a function of (A) $[C_{10}mim][BF_4]$, (B) $[C_{10}mim][Br]$, and (C) $[C_{10}mim][Cl]$ concentration.

Based on this study, we can accomplish that the interaction between CIP and ILs is spontaneous and stabilizes largely by a combination of hydrogen bond and hydrophobic and electrostatic forces.[52,55]

2.2. Time-Resolved Fluorescence Decay Studies. To exploit the photochemical nature of drug and IL interactions, we performed a fluorescence lifetime decay study. Fluorescence decay is the most reliable technique to check the
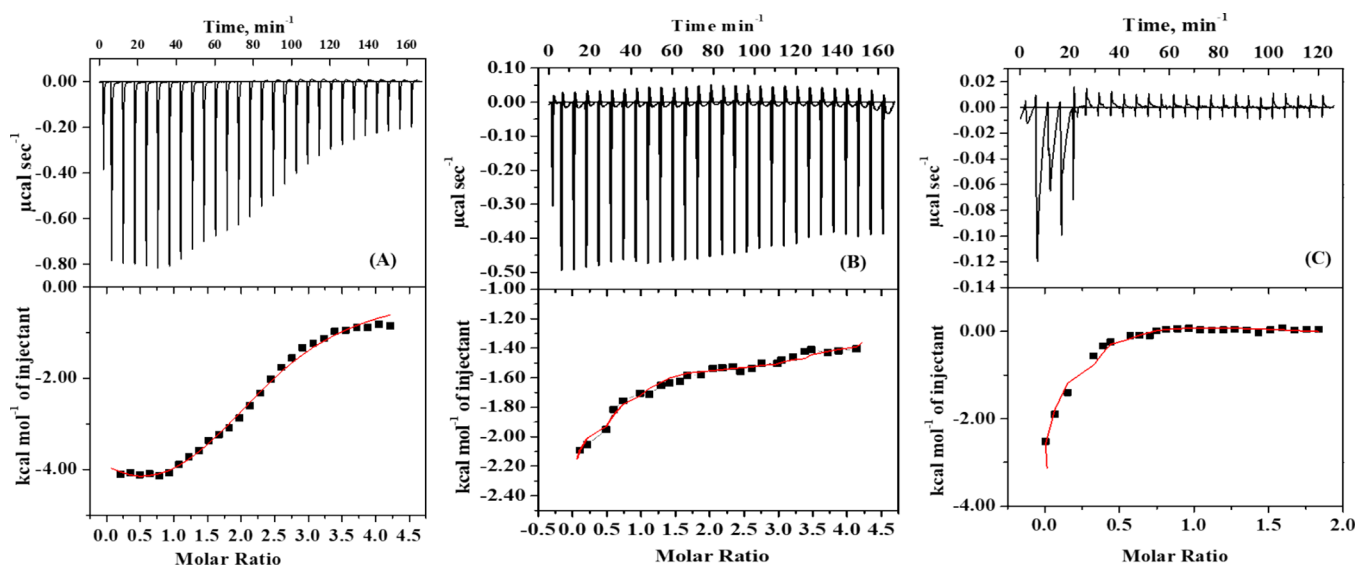
Figure 5. Isothermal calorimetric binding of CIP with titration of (A) $[C_{10}mim][BF_4]$, (B) $[C_{10}mim][Br]$, and (C) $[C_{10}mim][Cl]$ and their respective calorimetric responses.

molecular dynamics of drug molecules in the presence of ILs in the excited state. The alteration in fluorescence lifetime helps in getting a clear understanding about the inflection of photophysical properties, i.e., radiative and nonradiative, brought about by the interaction of a drug molecule. Fluorescence decay profiles of the drug generated from time-correlated single photon counting (TCSPC) in the absence and presence of IL are shown in Figure 3, and the corresponding decay values are listed in Tables S1−S3. The decays were found to be triexponential, which is in complete agreement with the earlier report.[56] The individual lifetimes (τ_1, τ_2, and τ_3) and the respective amplitudes (α_1, α_2, and α_3) are given in Tables S1−S3, along with the average lifetime (τ_{avg}) of CIP in the absence and presence of all three ILs calculated by using eq 10. The native drug, CIP (20 μM), has τ_0 equal to 1.41 ns in aqueous medium, which is almost similar to the previously reported literature.[56,57] From Tables S1−S3, it can be observed that the τ_{avg} value of CIP is enhanced slightly in the presence of the three ILs with increasing concentrations. The change in the τ_{avg} value of CIP in the presence of ILs suggests the complex formation between CIP−IL. Further, the τ_{avg} values were utilized to gain insight into the possible quenching mechanism involved in the interaction. Since the τ_{avg} value of CIP in the presence of the three ILs did not change quite significantly, the involvement of a static quenching mechanism is observed in the system. These results support the results obtained from the steady-state fluorescence study. It can be ascertained that the long-chain surface active imidazolium-based ILs have an effect on the decays of CIP as shown in Figure 3, with similar results being reported by Chen et al.[58] The enhancement in the average lifetime of the drug with increasing concentrations of ILs can be attributed to the intermolecular H-bonding between the drug molecules and IL micelles. In the protic solvent, multiple H-bonds exist between carboxylic and keto groups of CIP and ILs' head groups.[56] The encapsulation of the drug in the micellar core could bring about a decrease of nonradiative decay channels by minimizing the vibrational/rotational degrees of freedom.[59,60]

2.3. UV−Visible Study. Absorption spectroscopy is an important technique for studying the interaction between the

drug and IL. To validate the steady-state fluorescence and lifetime decay study of CIP and IL interactions, we contemplated the electronic absorption experiment. For this purpose, we investigated the absorption spectra of CIP (20 μM) in the presence of all the three ILs, $[C_{10}mim][BF_4]$, $[C_{10}mim][Br]$, and $[C_{10}mim][Cl]$. The spectra of CIP were scanned in the range of 230−400 nm in the absence and presence of ILs. The aqueous solution of CIP exhibited an intense peak at 274 nm (λ_{max}) and a weak absorption band at 332 nm.[61] No such absorption peaks were observed for ILs in this range. The absorption band of CIP at 274 nm is due to $\pi−\pi^*$ transition, while that at the longer wavelength is due to $n−\pi^*$ transition.[56] Figure 4A−C shows the absorption spectra of CIP in the presence of the ILs $[C_{10}mim][BF_4]$, $[C_{10}mim]$-[Br], and $[C_{10}mim][Cl]$ in increasing concentrations. The absorption spectra of the drug increases in the presence of ILs, revealing the complexation between CIP and ILs. In addition, we have observed a red shift (274 to 278 nm) and blue shift (332 to 328 nm) of 4 nm each in first and second spectral bands, respectively, upon the addition of $[C_{10}mim][BF_4]$ and $[C_{10}mim][Br]$. It signifies that upon interaction of the drug molecules with the ILs, they entered the more hydrophobic region from the aqueous region and showed the spectral red shift in its absorption maxima. Meanwhile, in the case of $[C_{10}mim][Cl]$, no such shift was observed in its absorption spectra (Figure 4 C). Like fluorescence emission of CIP with $[C_{10}mim][Cl]$, absorption of the drug does not show any spectral shift in the presence of $[C_{10}mim][Cl]$, indicating that it has no effect on the ground state but an extensive effect on the excited state. This study suggests that the ground-state complex formation between CIP and ILs is mostly favored by $[C_{10}mim][BF_4]$ and $[C_{10}mim][Br]$. The different behavior of IL interactions with CIP may be due to the changes in the nature of the chromophore, polarizability, charge distribution, size, etc. The change in the spectra shows the interaction of the drug with ILs and formation of a new complex between CIP and ILs. Recently, Senthilkumar et al. studied the solubilization and interaction of a drug with mixed Pluronic micelles by UV−visible spectroscopy and steady-state fluorescence techniques.[62,63]

Table 2. ITC-Derived Profile for the Interaction of CIP in the Presence of $[C_{10}mim][BF_4]$, $[C_{10}mim][Br]$, and $[C_{10}mim][Cl]$

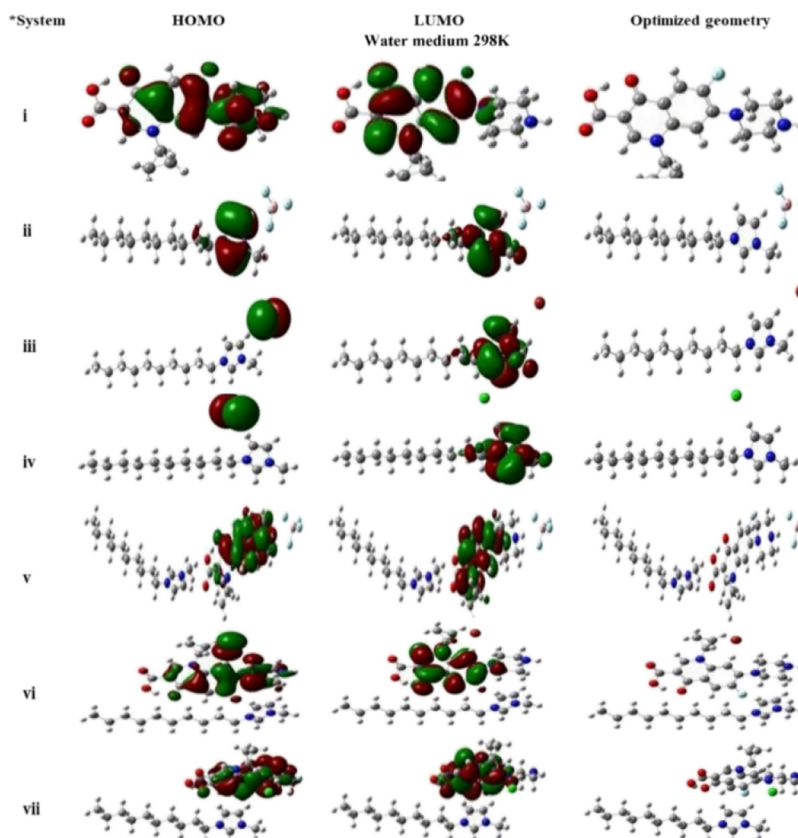| parameter	CIP-$[C_{10}mim][BF_4]$	CIP-$[C_{10}mim][Br]$	CIP-$[C_{10}mim][Cl]$
ΔH (kJ mol^{-1})	−21.02	−11.93	−17.89
ΔS (J mol^{-1})	108.78	234.30	14.22
ΔG (kJ mol^{-1})	−28.76	−28.61	−18.90
K_a (L mol^{-1})	1.20	1.06	0.084

Figure 6. Frontier molecular orbitals (HOMO and LUMO) and optimized geometry of CIP, ILs, and their complexation in the gaseous state at 298 K.

2.4. Isothermal Titration Calorimetry Study.

Isothermal titration calorimetry (ITC) is a powerful technique widely used to measure the heat absorbed or generated in interactions between two molecules. It provides important thermodynamic parameters upon the interactions of a drug with ILs as well as other molecules due to its ability to locate the energy absorbed or released upon interaction of individual molecules with one another. To determine the thermodynamic parameters and binding stoichiometries of the drug−IL interactions, ITC measurements were performed for CIP and IL interaction systems. For each measurement, IL was taken in a syringe and titrated into the cell containing the drug (CIP). The corresponding calorimetry responses were recorded, and they are shown in Figure 5. The top panel in this figure displays the raw data as power (μcal s^{-1}) vs time. The lower panel of the figure shows the raw data in power standardized to the number of the injectant (kcal mol^{-1}) vs its molar ratio during the injections of the ILs with the drug (CIP) in the cell. Figure 5A−C shows the thermograms of CIP and its interaction with the three ILs, i.e., $[C_{10}mim][BF_4]$, $[C_{10}mim][Br]$, and $[C_{10}mim][Cl]$, and CIP, which yielded the thermodynamic parameters. Table 2 shows the complete profile of thermodynamic parameters obtained from ITC measurements, which

signifies that the interaction between CIP and ILs was spontaneous, as observed from the free energy values.

The enthalpy change (ΔH) of the CIP-$[C_{10}mim][BF_4]$ interaction is more negative as compared to CIP-$[C_{10}mim]$-$[Br]$ and CIP-$[C_{10}mim][Cl]$ binding. The higher enthalpy change indicates the greater interaction of CIP with ligands through strong hydrophobic interactions. The enthalpograms obtained for the CIP-$[C_{10}mim][Cl]$ complex show not any major change compared to the enthalpograms of CIP-$[C_{10}mim][BF_4]$ and CIP-$[C_{10}mim][Br]$ complexes. This result can be ascribed to the difference in structural change in the counterion. The enthalpy scales of all three ILs with CIP are different, emphasizing the influence of the counterion in the 1-decyl-3-methylimidazolium cation when interacting with the drug. From Table 2, it is seen that the K_a value of CIP-$[C_{10}mim][BF_4]$ interaction is the highest, which suggests that $[C_{10}mim][BF_4]$ has greater binding affinity with CIP than $[C_{10}mim][Br]$ and $[C_{10}mim][Cl]$. The results indicate that $[C_{10}mim][BF_4]$ has more binding affinity with the drug owing to the presence of four highly electronegative fluorine atoms involved in attraction with the carboxylic and carbonyl moieties of CIP. Similar results have been proposed by Ghosh et al. for the interaction of CIP with surfactants SDS
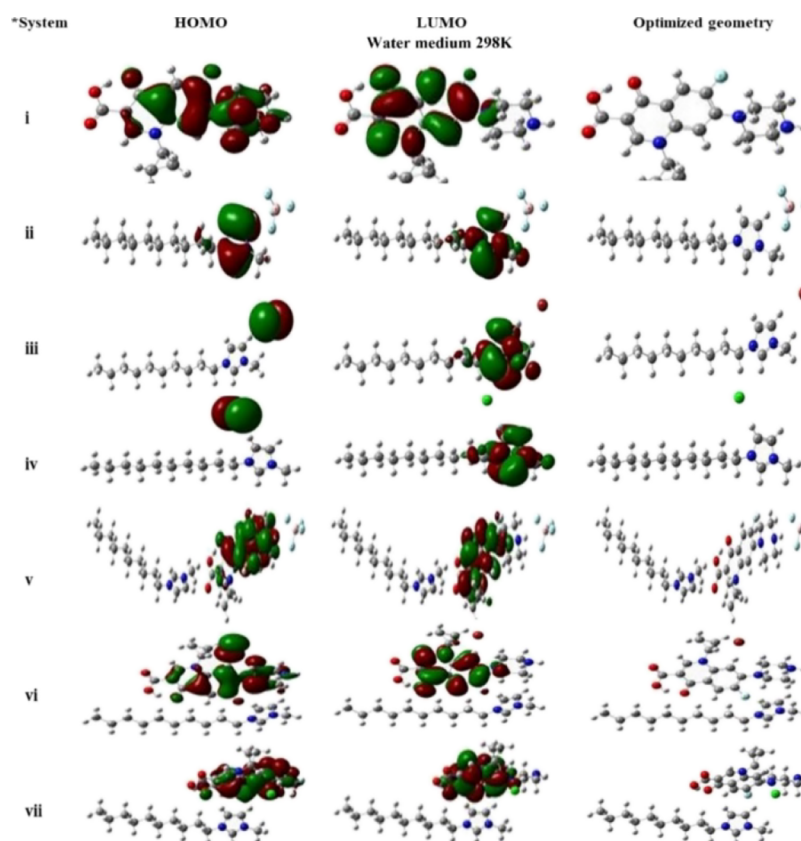
Figure 7. Frontier molecular orbitals (HOMO and LUMO) and optimized geometry of CIP, ILs, and their complexation in the water medium at 298 K.

and CTAB, and they agreed that electrostatic attraction plays a vital role in the interaction between CIP and SDS/CTAB molecules in aqueous medium.[39] The associated interaction parameters for all of the IL−CIP interactions are summarized in Table 2, and they revealed that the binding processes are spontaneous in nature and entropy-driven. The change in enthalpy and entropy values signifies that the bimolecular interaction between the drug and ILs is enthalpy−entropy-dependent.

2.5. Density Functional Theory (DFT). The molecular orbitals (HOMO and LUMO) play a vital role in interpreting the stability and reactivity of a molecule upon its interaction with other species. HOMO and LUMO are characterized by their electron-donating and electron-withdrawing ability, respectively.[1,64] A high HOMO value implies that the molecule is a good electron donor, whereas a lower value denotes its weak electron-donating capacity. Therefore, the physicochemical descriptors and thermodynamic parameters of the ILs, CIP, and their complexes were calculated at different temperatures, and they are given in the Supporting Information (Tables S4 and S5). To predict the chemical reactivity and stability of a molecule, we calculated the band gap ($\Delta E = E_{\text{LUMO}} - E_{\text{HOMO}}$) of all the complexes as given in Table S5. The energy gap between HOMO and LUMO has a substantial effect on the bioactivity and intermolecular charge transfer. The higher the energy gap, the lesser is the reactivity of the complex.[65] Further, DFT calculations were also performed for the drug and IL interaction at different temperatures and media (gas and water). Figures 6 and 7 depict the HOMO and LUMO and optimize the geometry of CLP, ILs, and their compensation in gaseous and water media,

respectively, at 298.15 K, while that for an elevated temperature is given in Figure S1. These charge density plots contribute to identifying the atoms involved in the interactions between the ligand and the receptor. At 298.15 K, in the gaseous state, the electron density is on the anion in the HOMO and on the ring of the cation in the LUMO. But in the case of the drug, the electron density is well delocalized throughout the molecule. Further, on considering the complexes of the drug with the imidazolium cation of the ILs, the electron density is mainly localized on the drug in both the HOMO and LUMO.

From Table S5, the values of ΔE were calculated and found to be higher for CIP-[C_{10}mim][BF_4] as compared to those of CIP-[C_{10}mim][Br] and CIP-[C_{10}mim][Cl] complexes, suggesting the higher stability of CIP with [C_{10}mim][BF_4] at 298 K and the maximum reactivity for CIP-[C_{10}mim][Br]. With increasing temperature, the value of ΔE for CIP-[C_{10}mim]-[BF_4] increases, revealing a high stability of the complex, even at elevated temperature. A similar trend in results was obtained when water was used as the medium but with a slight increase in the values of ΔE, indicating the higher stability of the complex in the water medium than that in the gaseous medium.[66] With water as the medium, the electron density in the ILs does not have a regular pattern in HOMO as well as in LUMO. In the case of [C_{10}mim][BF_4], the electron density is on the ring in HOMO and LUMO. Meanwhile, in the case of [C_{10}mim][Br] and [C_{10}mim][Cl], different patterns are observed.

In HOMO, the electron density is on the anion, while in LUMO, the electron density is localized on the ring of the cation of the respective ILs. Similar results were obtained at

different temperatures (308, 318, and 328 K) as shown in Figure S1.

Further, thermodynamic energies of the drug, ILs, and their complexes are given in Table S4. From Table S4, the zero-point energy, optimization energy, thermal energy, enthalpy, etc., of the ILs, drug, and their complexes have been assessed in the gaseous state as well as in water at different temperatures. All the energies of ILs, drug, and their complexes are negative. The negative energies of the IL−CIP complex suggest feasible interaction between IL and CIP, which validate our experimental results. Further, for a better understanding of the formation of the complexes, the change in free energy was calculated, and it is given in Table 3. In Table 3, the values are

Table 3. Change in Free Energy for the Formation of the Complexes in the Gaseous State and in Water at Various Temperatures (298, 308, 318, and 328 K)

complex	temp. (K)	ΔG (Hartree per particle)		ΔG(kcal/mol)	
		gaseous	water	gaseous	water
CIP-$[C_{10}mim][BF_4]$	298	−0.03	0.02	−18.82	12.55
CIP-$[C_{10}mim][Br]$		−0.01	0.02	−6.27	12.55
CIP-$[C_{10}mim][Cl]$		−0.01	0.01	−6.27	6.27
CIP-$[C_{10}mim][BF_4]$	308	−0.01	0	−6.27	0
CIP-$[C_{10}mim][Br]$		−0.02	0.01	−12.5	6.27
CIP-$[C_{10}mim][Cl]$		−0.01	0.02	−6.27	12.55
CIP-$[C_{10}mim][BF_4]$	318	−0.01	0	−6.27	0
CIP-$[C_{10}mim][Br]$		−0.01	0.02	−6.27	12.55
CIP-$[C_{10}mim][Cl]$		−0.01	0.01	−6.27	6.27
CIP-$[C_{10}mim][BF_4]$	328	−0.02	0.01	−12.55	6.27
CIP-$[C_{10}mim][Br]$		−0.01	0.01	−6.27	6.27
CIP-$[C_{10}mim][Cl]$		−0.02	0.01	−12.55	6.27

calculated in Hartree per particle (ΔG) and, since the variation in free energies for different complexes appeared very small, the values are shown in kcal/mol. From these ΔG values, it can be seen that the change in the free energy for the complexes at 298.15, 308.15, 318.15, and 328.15 K in the gaseous system is negative, while for that in water, ΔG values for the complexes at different temperatures were not negative. There is no difference in the change in free energy for the formation of a complex on considering bromide and chloride as anions in the imidazolium cation, but a minor change is observed for tetrafluoroborate as an anion in the IL. The negative values of thermal enthalpy in Table S4 depict that the complex formation of ILs with the CIP is exothermic.[67]

From the values mentioned in Table S5 (Supporting Information), various physiochemical parameters, viz., $E_{HOMO} - E_{LUMO}$, $E_{HOMO} + E_{LUMO}$, electronegativity (χ), chemical hardness (η), chemical potential (μ), softness (S), and global electrophilicity index (ω), were evaluated from the energies of frontier molecular orbitals according to eqs 4−8.

$$\mu = (E_{HOMO} + E_{LUMO})/2 \tag{4}$$

$$\chi = -(E_{HOMO} + E_{LUMO})/2 \tag{5}$$

$$\eta = (E_{LUMO} + E_{HOMO})/2 \tag{6}$$

$$S = (1/2\eta) \tag{7}$$

$$\omega = \left(\frac{\mu^2}{2\eta}\right) \tag{8}$$

The higher energy of the HOMO of a molecule indicates a higher potency or its ability to donate the electron and its higher reactivity. Therefore, $[C_{10}mim][BF_4]$ was found to be the most reactive in gaseous as well as in water medium at 298, 308, 318, and 328 K. Further, the lower energy of LUMO clearly indicates its higher tendency to accept electrons and, thus, its reactivity will be higher. The energy difference between the HOMO and the LUMO is an important parameter for the reactivity of a molecule. Lesser difference in the energies of HOMO and LUMO of a molecule means that its chemical reactivity will be higher.[28,68] From Table S5, the values of μ are observed to be negative for each case, indicating the good stability and formation of a stable complex between the ligand and the receptor with maximum stability for CIP-$[C_{10}mim][BF_4]$ in gaseous as well as water medium and at elevated temperatures too.[69] The molecular reactivity and stability can also be established in terms of the total chemical hardness and chemical softness. Hardness leads to high resistance in a change of electronic distribution amid a chemical reaction and vice versa for softness. Molecules possessing a large band gap usually exhibit hardness and, in turn, are more stable.[65] Also, the polarizability can be related to chemical hardness and softness. The greater the softness, the higher the polarizability will be, and so the softness of $[C_{10}mim][Br]$ is maximum among the three complexes in the gaseous state at all the four temperatures and hence exhibits maximum polarizability, whereas for the water medium, all three demonstrate similar softness and, consequently, polarizability. Hence, from the results obtained through DFT, the most stable complex can be derived as that of CIP-$[C_{10}mim][BF_4]$. The outcomes from DFT yield a better understanding of the reactivity of drug molecules with the ligands, and their applications in the pharmaceutical industry can be explored further, especially with ionic liquids for utilizing these as better therapeutic candidates.[70]

3. CONCLUSIONS

The present study investigated the interaction of CIP with three surface active ILs ($[C_{10}mim][BF_4]$, $[C_{10}mim][Br]$, and $[C_{10}mim][Cl]$) by employing various techniques. The fluorescence spectroscopy study revealed that the emission spectra of CIP quenched in the presence of all three ILs, attributed to the complex formation between CIP and ILs. The complex formation was further confirmed by time-resolved fluorescence results and suggested the involvement of a static quenching mechanism. The proficiency of quenching for the CIP emission was different for each IL, which may be due to the structural differences in the counterion. The associated binding and thermodynamic parameters calculated from the fluorescence emission were ascribed to spontaneous complex formation between CIP and ILs. The complexation between CIP-$[C_{10}mim][BF_4]$ is stronger than that between CIP-$[C_{10}mim][Br][C_{10}mim][Cl]$. Further, interaction of CIP with ILs was confirmed by UV−visible spectroscopic studies, which indicated the strong binding of CIP with ILs. An enhancement in the absorption spectra of CIP in the presence of ILs was observed due to the ground-state complex formation between the drug and ILs. Both the emission and absorption spectroscopic results supported the strong interaction between CIP and ILs. ITC results showed that the CIP−IL interaction is thermodynamically feasible and enthalpy-driven. The complexation of the drug and ILs was

further validated by classical DFT calculation in gaseous and water media.

4. MATERIALS AND METHODS

4.1. Materials. The chemicals, namely, 1-decyl-3-methyl-imidazolum tetrafluoroborate, 1-decyl-3-methylimidazolium bromide, 1-decyl-3-methylimidazolum chloride, and the drug ciprofloxacin were procured from Sigma-Aldrich, USA. The drug solution was prepared in double-distilled water and stirred for 5 min to ensure complete mixing. The final concentration of the drug solution (ε = 35,900 $M^{-1}cm^{-1}$) was assessed using an Analytik Jena Specord-250 UV–vis spectrophotometer at 274 nm using Beer–Lambert law.[17] The structures of ILs and the drug are given in Scheme 1.

Scheme 1. Structures of ILs and the Drug Used in the Study
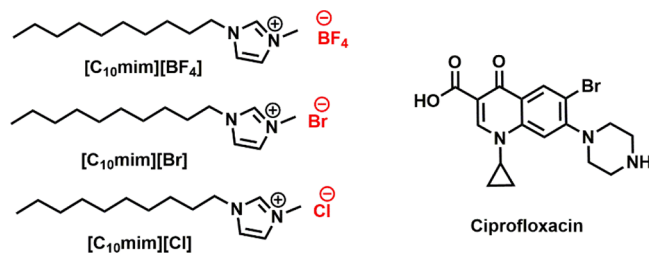
4.2. Methods. *4.2.1. Steady-State Fluorescence Spectroscopy.* Steady-state fluorescence spectroscopy measurements were performed on a Cary Eclipse Fluorescence spectrophotometer (Agilent Technology, California, United States) using a quartz cuvette of 1 cm in path length at 298.15 K. The emission spectra of CIP were excited at 274 nm (λ_{max} = 274 nm), and the spectra were scanned in the range of 350–580 nm setting emission/excitation band widths at 5 nm/5 nm.[45] The concentration of the drug (20 μM) was kept constant throughout the experiment.

4.2.2. Time-Resolved Fluorescence Spectroscopy. Lifetime measurement study was performed on a time-resolved spectrophotometer (Horiba Scientific, Delta Fle*x* Jobin Yvon, technology, Glasgow, UK) equipped with a nanosecond pulse, λ_{max} head at 284 nm, and λ_{max} head at 450 nm at 298 K. The lifetime decays were measured to 10,000 counts with a band pass of 8 nm. The emission lifetime of the drug was measured by using time-correlated single photon counting (TCSPC) at room temperature. The instrument response function (IRF) was taken by using a standard probe, LUDOX solution, with a calibration time of 114 ps. The decay curves were fitted to the triexponential iterative program and analyzed by decay analysis software (Horiba-EzTime software).[46] The goodness of fit was arbitrated in terms of χ^2 and weighted residuals. The experimental method of time-resolved fluorescence was the same as that previously defined in the literature.[47−49] For each measurement, an aqueous solution of drug was excited at 284 nm (the excitation source used was 284 nm) at various concentrations of ILs and the data were fitted according to eq 9. The concentration of the drug was kept at 20 μM throughout the experiment.

$$f(t) = \sum_{i=1}^{n} a_i \exp\left\langle \frac{-\tau}{\tau_i} \right\rangle \tag{9}$$

where τ_i is the decay time, a_i is the relative contribution of the components at t = 0, and n is the number of decay time fit. The average lifetimes (τ_{avg}) for triexponential fitting of the drug solution at various concentrations of ILs were estimated from the decay time (τ) and the relative amplitude (α) according to eq 10.

$$\langle \tau_{avg} \rangle = \frac{\sum \alpha_i \tau_i^2}{\sum \alpha_i \tau_i} \tag{10}$$

4.2.3. UV−Visible Spectroscopy. The UV−visible absorption study was performed on an Analytik Jena Specord-250 spectrophotometer with quartz cells of 1 cm in path length at 298.15 K. All absorption spectra of CIP in the presence and absence of the ILs were scanned from the 200 to 400 nm range. A 20 μM drug concentration was used for all UV−vis absorbance experiments.

4.2.4. Isothermal Titration Calorimetry (ITC). The enthalpy−entropy change assisting the titration of IL solutions with CIP was determined by a Malvern MicroCal VP-ITC, UK, at 298.15 K. All of the measurement solutions were degassed before each experiment to avoid the presence of bubbles during the experiment. The titrations were performed by adding ILs [C$_{10}$mim][BF$_4$], [C$_{10}$mim][Br], and [C$_{10}$mim]-[Cl] as ligands into the cell where the drug CIP was placed. The concentration ratio of the receptor and ligand was taken to be 1:30 (in μM). In each experiment, the ligand was suspended in the same buffer as CIP and 10 μL aliquots were injected at 260 s. Experimental raw data were analyzed by using Origin software by a three-step sequential binding model, which could fit the data to produce various thermodynamic binding parameters including enthalpy change (ΔH), entropy change (ΔS), and association constant (K_a). By utilizing these parameters, Gibbs free energy change (ΔG) and binding constant (K_a) were calculated from eq 11.

$$\Delta G = \Delta H - T\Delta S \tag{11}$$

where T is the temperature in Kelvin.

4.2.5. Density Functional Theory (DFT). To explore the electronic structures and the interactions between the ILs and CIP, a DFT study was performed. The structures of ILs, drug, and IL−drug complexes (IL−CIP) and the representation of HOMO and LUMO were optimized and developed in the gas phase and water phase by using the B3LYP/6-311G (d, p) basis set on Gaussian 09 software according to the classical DFT model. The optimization energy, zero-point energy, thermal energy, thermal enthalpy, and free energy of the ILs, drug, and their complexes were investigated at different temperatures (298.15, 308.15, 318.15, and 328.15K).

■ ASSOCIATED CONTENT

ⓈI Supporting Information

The Supporting Information is available free of charge at https://pubs.acs.org/doi/10.1021/acsomega.3c05100.

> DFT analysis at different temperatures and time-resolved fluorescence results (PDF)

■ AUTHOR INFORMATION

Corresponding Authors

> **Rajan Patel** − *Biophysical Chemistry Laboratory, Centre for Interdisciplinary Research in Basic Sciences, Jamia Millia Islamia, New Delhi 110025, India;* ● orcid.org/0000-0002-3811-2898; Phone: +91 8860634100; Email: rpatel@jmi.ac.in; Fax: +91 11 26983409

Abeer A. Ageeli − *Department of Chemistry, Faculty of Science, Jazan University, Jazan 45142, Saudi Arabia;* Email: abeerali@jazanu.edu.sa

Authors

Abrar Siddiquee − *Biophysical Chemistry Laboratory, Centre for Interdisciplinary Research in Basic Sciences, Jamia Millia Islamia, New Delhi 110025, India*

Zahoor Parray − *Department of Chemistry, IIT Delhi, New Delhi 110016, India;* orcid.org/0000-0001-5998-7100

Aashima Anand − *Biophysical Chemistry Laboratory, Centre for Interdisciplinary Research in Basic Sciences, Jamia Millia Islamia, New Delhi 110025, India*

Shadma Tasneem − *Department of Chemistry, Faculty of Science, Jazan University, Jazan 45142, Saudi Arabia*

Nazim Hasan − *Department of Chemistry, Faculty of Science, Jazan University, Jazan 45142, Saudi Arabia*

Waleed M. Alamier − *Department of Chemistry, Faculty of Science, Jazan University, Jazan 45142, Saudi Arabia*

Farooq Ahmad Wani − *Biophysical Chemistry Laboratory, Centre for Interdisciplinary Research in Basic Sciences, Jamia Millia Islamia, New Delhi 110025, India*

Prashant Singh − *Department of Chemistry, ARSD College, Delhi University, New Delhi 110021, India*

Complete contact information is available at:
https://pubs.acs.org/10.1021/acsomega.3c05100

Notes

The authors declare no competing financial interest.

■ REFERENCES

(1) Singla, P.; Singh, O.; Sharma, S.; Betlem, K.; Aswal, V. K.; Peeters, M.; Mahajan, R. K. Temperature-Dependent Solubilization of the Hydrophobic Antiepileptic Drug Lamotrigine in Different Pluronic Micelles-A Spectroscopic, Heat Transfer Method, Small-Angle Neutron Scattering, Dynamic Light Scattering, and in Vitro Release Study. *ACS Omega* **2019**, *4* (6), 11251−11262.

(2) Wang, C.; Chopade, S. A.; Guo, Y.; Early, J. T.; Tang, B.; Wang, E.; Hillmyer, M. A.; Lodge, T. P.; Sun, C. C. Preparation, characterization, and formulation development of drug−drug protic ionic liquids of diphenhydramine with ibuprofen and naproxen. *Mol. Pharmaceutics* **2018**, *15* (9), 4190−4201.

(3) Nazar, M. F.; Mukhtar, F.; Chaudry, S.; Ashfaq, M.; Mehmood, S.; Asif, A.; Rana, U. A. Biophysical probing of antibacterial gemifloxacin assimilated in surfactant mediated molecular assemblies. *J. Mol. Liq.* **2014**, *200*, 361−368.

(4) Karagianni, A.; Malamatari, M.; Kachrimanis, K. Pharmaceutical cocrystals: new solid phase modification approaches for the formulation of APIs. *Pharmaceutics* **2018**, *10* (1), 18.

(5) Rodriguez-Aller, M.; Guillarme, D.; Veuthey, J.-L.; Gurny, R. Strategies for formulating and delivering poorly water-soluble drugs. *J. Drug Delivery Sci. Technol.* **2015**, *30*, 342−351.

(6) Tran, T. T.; Tran, P. H. Nanoconjugation and encapsulation strategies for improving drug delivery and therapeutic efficacy of poorly water-soluble drugs. *Pharmaceutics* **2019**, *11* (7), 325.

(7) Md Moshikur, R.; Chowdhury, M. R.; Moniruzzaman, M.; Goto, M. Biocompatible ionic liquids and their applications in pharmaceutics. *Green Chem.* **2020**, *22* (23), 8116−8139.

(8) Sahbaz, Y.; Nguyen, T.-H.; Ford, L.; McEvoy, C. L.; Williams, H. D.; Scammells, P. J.; Porter, C. J. Ionic liquid forms of weakly acidic drugs in oral lipid formulations: preparation, characterization, in vitro digestion, and in vivo absorption studies. *Mol. Pharmaceutics* **2017**, *14* (11), 3669−3683.

(9) Adawiyah, N.; Moniruzzaman, M.; Hawatulaila, S.; Goto, M. Ionic liquids as a potential tool for drug delivery systems. *Med. Chem. Commun.* **2016**, *7* (10), 1881−1897.

(10) Talele, P.; Choudhary, S.; Kishore, N. Understanding thermodynamics of drug partitioning in micelles and delivery to proteins: Studies with naproxen, diclofenac sodium, tetradecyltrimethylammonium bromide, and bovine serum albumin. *J. Chem. Thermodyn.* **2016**, *92*, 182−190.

(11) Patel, A. A.; Dave, R. H. Development and characterization of innovative liquid salt based formulations of sparingly soluble drugs. *Int. J. Pharm. Sci. Res.* **2015**, *6*, 2316−2327.

(12) Kucherov, F. A.; Egorova, K. S.; Posvyatenko, A. V.; Eremin, D. B.; Ananikov, V. P. Investigation of cytotoxic activity of mitoxantrone at the individual cell level by using ionic-liquid-tag-enhanced mass spectrometry. *Anal. Chem.* **2017**, *89* (24), 13374−13381.

(13) Hu, X.; Zeng, Z.; Zhang, J.; Wu, D.; Li, H.; Geng, F. Molecular dynamics simulation of the interaction of food proteins with small molecules. *Food Chem.* **2022**, No. 134824, DOI: 10.1016/j.foodchem.2022.134824.

(14) Li, M.; Zhou, D.; Wu, D.; Hu, X.; Hu, J.; Geng, F.; Cheng, L. Comparative analysis of the interaction between alpha-lactalbumin and two edible azo colorants equipped with different sulfonyl group numbers. *Food Chem.* **2023**, *416*, No. 135826.

(15) Frizzo, C. P.; Wust, K.; Tier, A. Z.; Beck, T. S.; Rodrigues, L. V.; Vaucher, R. A.; Bolzan, L. P.; Terra, S.; Soares, F.; Martins, M. A. Novel ibuprofenate-and docusate-based ionic liquids: emergence of antimicrobial activity. *RSC Adv.* **2016**, *6* (102), 100476−100486.

(16) Egorova, K. S.; Ananikov, V. P. Fundamental importance of ionic interactions in the liquid phase: A review of recent studies of ionic liquids in biomedical and pharmaceutical applications. *J. Mol. Liq.* **2018**, *272*, 271−300.

(17) Siddiquee, M. A.; Patel, R.; Saraswat, J.; Khatoon, B. S.; ud din Parray, M.; Wani, F. A.; Khan, M. R.; Busquets, R. Interfacial and antibacterial properties of imidazolium based ionic liquids having different counterions with ciprofloxacin. *Colloids Surf., A* **2021**, *629*, No. 127474.

(18) Chen, B.; Li, K.; Sun, H.; Jiang, L.; Yang, M.; Song, Y. Promoting effect of common marine cations on hydrate dissociation and structural evolution under a static electric field. *J. Phys. Chem. B* **2023**, *127* (3), 698−709.

(19) Mahajan, S.; Sharma, R.; Mahajan, R. K. An investigation of drug binding ability of a surface active ionic liquid: micellization, electrochemical, and spectroscopic studies. *Langmuir* **2012**, *28* (50), 17238−17246.

(20) Miwa, Y.; Hamamoto, H.; Ishida, T. Lidocaine self-sacrificially improves the skin permeation of the acidic and poorly water-soluble drug etodolac via its transformation into an ionic liquid. *Eur. J. Pharm. Biopharm.* **2016**, *102*, 92−100.

(21) Egorova, K. S.; Gordeev, E. G.; Ananikov, V. P. Biological activity of ionic liquids and their application in pharmaceutics and medicine. *Chem. Rev.* **2017**, *117* (10), 7132−7189.

(22) Mahmood, H.; Moniruzzaman, M.; Yusup, S.; Welton, T. Ionic liquids assisted processing of renewable resources for the fabrication of biodegradable composite materials. *Green Chem.* **2017**, *19* (9), 2051−2075.

(23) Behera, K.; Om, H.; Pandey, S. Modifying properties of aqueous cetyltrimethylammonium bromide with external additives: ionic liquid 1-hexyl-3-methylimidazolium bromide versus cosurfactant n-hexyltrimethylammonium bromide. *J. Phys. Chem. B* **2009**, *113* (3), 786−793.

(24) Behera, K.; Pandey, S. Modulating properties of aqueous sodium dodecyl sulfate by adding hydrophobic ionic liquid. *J. Colloid Interface Sci.* **2007**, *316* (2), 803−814.

(25) Banjare, M. K.; Behera, K.; Satnami, M. L.; Pandey, S.; Ghosh, K. K. Self-assembly of a short-chain ionic liquid within deep eutectic solvents. *RSC Adv.* **2018**, *8* (15), 7969−7979.

(26) Saraswat, J.; Wani, F. A.; Dar, K. I.; Rizvi, M. M. A.; Patel, R. Noncovalent conjugates of ionic liquid with antibacterial peptide melittin: an efficient combination against bacterial cells. *ACS Omega* **2020**, *5* (12), 6376−6388.

(27) Khan, A. B.; Wani, F. A.; Dohare, N.; Parray, M. u. D.; Singh, P.; Patel, R. Ionic liquid influenced synergistic interaction between amitriptyline hydrochloride and cetyltrimethylammonium bromide. *J. Chem. Eng. Data* **2017**, *62* (10), 3064−3070.

(28) Khan, A. B.; Ali, M.; Dohare, N.; Singh, P.; Patel, R. Micellization behavior of the amphiphilic drug promethazine hydrochloride with 1-decyl-3-methylimidazolium chloride and its thermodynamic characteristics. *J. Mol. Liq.* **2014**, *198*, 341−346.

(29) Tariq, M.; Freire, M. G.; Saramago, B.; Coutinho, J. A.; Lopes, J. N. C.; Rebelo, L. P. N. Surface tension of ionic liquids and ionic liquid solutions. *Chem. Soc. Rev.* **2012**, *41* (2), 829−868.

(30) Goossens, K.; Lava, K.; Bielawski, C. W.; Binnemans, K. Ionic liquid crystals: versatile materials. *Chem. Rev.* **2016**, *116* (8), 4643−4807.

(31) Bhat, A. R.; Wani, F. A.; Alzahrani, K. A.; Alshehri, A. A.; Malik, M. A.; Patel, R. Effect of rifampicin on the interfacial properties of imidazolium ionic liquids and its solubility therein. *J. Mol. Liq.* **2019**, *292*, No. 111347.

(32) Amaral, M.; Pereiro, A. B.; Gaspar, M. M.; Reis, C. P. Recent advances in ionic liquids and nanotechnology for drug delivery. *Nanomedicine* **2021**, *16* (1), 63−80.

(33) Pedro, S. N.; R Freire, C. S.; Silvestre, A. J. D.; Freire, M. G. The role of ionic liquids in the pharmaceutical field: An overview of relevant applications. *Int. J. Mol. Sci.* **2020**, *21* (21), 8298.

(34) Sintra, T. E.; Shimizu, K.; Ventura, S. P. M.; Shimizu, S.; Canongia Lopes, J. N.; Coutinho, J. A. P. Enhanced dissolution of ibuprofen using ionic liquids as catanionic hydrotropes. *Phys. Chem. Chem. Phys.* **2018**, *20* (3), 2094−2103.

(35) Hough, W. L.; Smiglak, M.; Rodríguez, H.; Swatloski, R. P.; Spear, S. K.; Daly, D. T.; Pernak, J.; Grisel, J. E.; Carliss, R. D.; Soutullo, M. D.; Davis, J. H., Jr.; Rogers, R. D. The third evolution of ionic liquids: active pharmaceutical ingredients. *New J. Chem.* **2007**, *31* (8), 1429−1436.

(36) Huang, W.; Wu, X.; Qi, J.; Zhu, Q.; Wu, W.; Lu, Y.; Chen, Z. Ionic liquids: Green and tailor-made solvents in drug delivery. *Drug discovery Today* **2020**, *25* (5), 901−908.

(37) Huang, Z.; Parikh, S.; Fish, W. P. Interactions between a poorly soluble cationic drug and sodium dodecyl sulfate in dissolution medium and their impact on in vitro dissolution behavior. *Int. J. Pharm.* **2018**, *535* (1−2), 350−359.

(38) Reid, J. E.; Prydderch, H.; Spulak, M.; Shimizu, S.; Walker, A. J.; Gathergood, N. Green profiling of aprotic versus protic ionic liquids: synthesis and microbial toxicity of analogous structures. *Sustainable Chemistry Pharmacy* **2018**, *7*, 17−26.

(39) Ghosh, R.; Hareendran, H.; Subramaniam, P. Adsorption of Fluoroquinolone Antibiotics at the Gas−Liquid Interface Using Ionic Surfactants. *Langmuir* **2019**, *35* (39), 12839−12850.

(40) Kurnik, I. S.; D'Angelo, N. A.; Mazzola, P. G.; Chorilli, M.; Kamei, D. T.; Pereira, J. F.; Vicente, A. A.; Lopes, A. M. Polymeric micelles using cholinium-based ionic liquids for the encapsulation and release of hydrophobic drug molecules. *Biomater. Sci.* **2021**, *9*, 2183−2196.

(41) Zhang, G.-F.; Liu, X.; Zhang, S.; Pan, B.; Liu, M.-L. Ciprofloxacin derivatives and their antibacterial activities. *Eur. J. Med. Chem.* **2018**, *146*, 599−612.

(42) Gorelik, E.; Masarwa, R.; Perlman, A.; Rotshild, V.; Abbasi, M.; Muszkat, M.; Matok, I. Fluoroquinolones and Cardiovascular Risk: A Systematic Review Meta-analysis and Network Meta-analysis. *Drug Saf.* **2019**, *42* (4), 529−538.

(43) Rehman, A.; Patrick, W. M.; Lamont, I. L. Mechanisms of ciprofloxacin resistance in Pseudomonas aeruginosa: new approaches to an old problem. *J. Med. Microbiol.* **2019**, *68* (1), 1−10.

(44) Rehman, A.; Jeukens, J.; Levesque, R. C.; Lamont, I. L. Gene-gene interactions dictate ciprofloxacin resistance in Pseudomonas aeruginosa and facilitate prediction of resistance phenotype from genome sequence data. *Antimicrob. Agents Chemother.* **2021**, *65* (7), No. e0269620.

(45) Muchohi, S. N.; Thuo, N.; Karisa, J.; Muturi, A.; Kokwaro, G. O.; Maitland, K. Determination of ciprofloxacin in human plasma using high-performance liquid chromatography coupled with fluorescence detection: Application to a population pharmacokinetics study in children with severe malnutrition. *J. Chromatogr. B* **2011**, *879* (2), 146−152.

(46) Singh, U. K.; Kumari, M.; Patel, R. Dynamics of cytochrome c in surface active ionic liquid: A study of preferential interactions towards denaturation. *J. Mol. Liq.* **2018**, *268*, 840−848.

(47) Maurya, N.; Maurya, J. K.; Singh, U. K.; Dohare, R.; Zafaryab, M.; Moshahid Alam Rizvi, M.; Kumari, M.; Patel, R. In vitro cytotoxicity and interaction of noscapine with human serum albumin: Effect on structure and esterase activity of HSA. *Mol. Pharmaceutics* **2019**, *16* (3), 952−966.

(48) Maurya, J. K.; Mir, M. U. H.; Singh, U. K.; Maurya, N.; Dohare, N.; Patel, S.; Ali, A.; Patel, R. Molecular investigation of the interaction between ionic liquid type gemini surfactant and lysozyme: A spectroscopic and computational approach. *Biopolymers* **2015**, *103* (7), 406−415.

(49) Patel, R.; Maurya, N.; Parray, M. u. d.; Farooq, N.; Siddique, A.; Verma, K. L.; Dohare, N. Esterase activity and conformational changes of bovine serum albumin toward interaction with mephedrone: Spectroscopic and computational studies. *J. Mol. Recognition* **2018**, *31* (11), No. e2734.

(50) Fotouhi, L.; Atoofi, Z.; Heravi, M. M. Interaction of ciprofloxacin with DNA studied by spectroscopy and voltammetry at MWCNT/DNA modified glassy carbon electrode. *Talanta* **2013**, *103*, 194−200.

(51) Khan, A. M.; Shah, S. S. Fluorescence spectra behavior of ciprofloxacin HCl in aqueous medium and its interaction with sodium dodecyl sulfate. *J. Dispersion Sci. Technol.* **2009**, *30* (7), 997−1002.

(52) Łuczak, J.; Markiewicz, M.; Thöming, J.; Hupka, J.; Jungnickel, C. Influence of the Hofmeister anions on self-organization of 1-decyl-3-methylimidazolium chloride in aqueous solutions. *J. Colloid Interface Sci.* **2011**, *362* (2), 415−422.

(53) García, C.; Oyola, R.; Piñero, L. E.; Arce, R.; Silva, J.; Sánchez, V. Substitution and Solvent Effects on the Photophysical Properties of Several Series of 10-Alkylated Phenothiazine Derivatives. *J. Phys. Chem. A* **2005**, *109* (15), 3360−3371.

(54) Kumar, P. K.; Jha, I.; Venkatesu, P.; Bahadur, I.; Ebenso, E. E. A comparative study of the stability of stem bromelain based on the variation of anions of imidazolium-based ionic liquids. *J. Mol. Liq.* **2017**, *246*, 178−186.

(55) Kumar, A.; Rani, A.; Venkatesu, P. A comparative study of the effects of the Hofmeister series anions of the ionic salts and ionic liquids on the stability of α-chymotrypsin. *New J. Chem.* **2015**, *39* (2), 938−952.

(56) Polishchuk, A.; Karaseva, E.; Emelina, T.; Karasev, V. Spectroscopic and photophysical properties of protonated forms of some fluoroquinolones in solutions. *J. Fluoresc.* **2012**, *22* (1), 373−379.

(57) Ferreira, M.; Gameiro, P. Ciprofloxacin metalloantibiotic: an effective antibiotic with an influx route strongly dependent on lipid interaction? *J. Membr. Biol.* **2015**, *248* (1), 125−136.

(58) Chen, I.-H.; Chen, Y.-F.; Liou, J.-H.; Lai, J.-T.; Hsu, C.-C.; Wang, N.-Y.; Jan, J.-S. Green synthesis of gold nanoparticle/gelatin/ protein nanogels with enhanced bioluminescence/biofluorescence. *Mater. Sci. Eng. C* **2019**, *105*, No. 110101.

(59) Mandal, S.; Banerjee, C.; Ghosh, S.; Kuchlyan, J.; Sarkar, N. Modulation of the photophysical properties of curcumin in nonionic surfactant (Tween-20) forming micelles and niosomes: a comparative study of different microenvironments. *J. Phys. Chem. B* **2013**, *117* (23), 6957−6968.

(60) Ghatak, C.; Rao, V. G.; Mandal, S.; Ghosh, S.; Sarkar, N. An understanding of the modulation of photophysical properties of curcumin inside a micelle formed by an ionic liquid: a new possibility of tunable drug delivery system. *J. Phys. Chem. B* **2012**, *116* (10), 3369−3379.

(61) Nazar, M. F.; Abid, M.; Danish, M.; Ashfaq, M.; Khan, A. M.; Zafar, M. N.; Mehmood, S.; Asif, A. Impact of L-leucine on controlled release of ciprofloxacin through micellar catalyzed channels in aqueous medium. *J. Mol. Liq.* **2015**, *212*, 142−150.

(62) Senthilkumar, M.; Sheelarani, B.; Joshi, R.; Dash, S. Solubilization and interaction of ciprofloxacin with pluronics and their mixed micelles. *New J. Chem.* **2019**, *43* (42), 16530−16537.

(63) Abrar Siddiquee, M.; Saraswat, J.; ud din Parray, M.; Singh, P.; Bargujar, S.; Patel, R. Spectroscopic and DFT study of imidazolium based ionic liquids with broad spectrum antibacterial drug levofloxacin. *Spectrochim. Acta Part A: Mol. Biomol. Spectrosc.* **2023**, *285*, No. 121803.

(64) Kumar, A.; Kumari, K.; Raman, A. P. S.; Jain, P.; Kumar, D.; Singh, P. An insight for the interaction of drugs (acyclovir/ ganciclovir) with various ionic liquids: DFT calculations and molecular docking. *J. Phys. Org. Chem.* **2022**, *35* (1), No. e4287.

(65) Ibrahim, A.; Ipinloju, N.; Aiyelabegan, A. O.; et al. Discovery of Potential Phytochemicals from Carica papaya Targeting BRCA-1 in Breast Cancer Treatment. *Appl. Biochem. Biotechnol.* **2023**, 1 DOI: 10.1007/s12010-023-04473-2.

(66) Kumar, A.; Kumari, K.; Singh, S.; Bahadur, I.; Singh, P. Noscapine anticancer drug designed with ionic liquids to enhance solubility: DFT and ADME approach. *J. Mol. Liq.* **2021**, *325*, No. 115159.

(67) Ekennia, A. C.; Onwudiwe, D. C.; Olasunkanmi, L. O.; Osowole, A. A.; Ebenso, E. E. Synthesis, DFT Calculation, and Antimicrobial Studies of Novel Zn(II), Co(II), Cu(II), and Mn(II) Heteroleptic Complexes Containing Benzoylacetone and Dithiocarbamate. *Bioinorg. Chem. App.* **2015**, *2015*, 1.

(68) Huang, Y.; Ouyang, D.; Ji, Y. The role of hydrogen-bond in solubilizing drugs by ionic liquids: A molecular dynamics and density functional theory study. *AIChE J.* **2022**, *68* (6), 17672.

(69) Jordaan, M. A.; Ebenezer, O.; Damoyi, N.; Shapi, M. Virtual screening, molecular docking studies and DFT calculations of FDA approved compounds similar to the non-nucleoside reverse transcriptase inhibitor (NNRTI) efavirenz. *Heliyon* **2020**, *6* (8), No. 04642.

(70) Saraswat, J.; Riaz, U.; Patel, R. In-silico study for the screening and preparation of ionic liquid-AVDs conjugate to combat COVID-19 surge. *J. Mol. Liq.* **2022**, *359*, No. 119277.